Determination of the Pressure Distortion Coefficient of Pressure Balances Using a Modified Experimental Method

Speaker/Author: Wladimir Sabuga
Physikalisch-Technische Bundesanstalt
Bundesallee 100, 38116 Braunschweig, Germany
Phone: +49 531 5923132; Fax: +49 531 592693132
wladimir.sabuga@ptb.de

Abstract

An experimental method for determining the pressure distortion coefficient of piston-cylinder assemblies of pressure balances based on piston fall rate and effective area measurements at variable jacket pressures is modified to extend it to non-cylindrical piston cylinders and compressible pressure-transmitting fluids and to accurately determine the analytical parameters required by the method. Applicability of the simplifying assumptions made so far is investigated, optimal parameters of a variable jacket pressure experiment are stated and procedures for the evaluation of experimental data are suggested. The effect of input information such as elastic properties of the assembly material and piston-cylinder gap profile on the uncertainty of the distortion coefficient is discussed. The modified method is applied to a 1 GPa piston-cylinder assembly and the results are compared with the those obtained by the finite element method.

1 Introduction

The accuracy of pressure measurements above approximately 50 MPa using pressure balances is limited by the knowledge of their pressure distortion coefficient (λ) describing the change of the effective area of the pressure balance (A_p) with pressure (p_0). Numerical methods, with the Finite Element Analysis (FEA) as the most efficient one, allow the radial elastic distortions, the pressure distribution in the gap and, thus, λ to be calculated if the properties of the piston-cylinder assembly and of the pressure-transmitting medium are known. The investigations of the last few years realized within the scope of a EUROMET research project [1] have demonstrated good agreement between the numerical methods of several European national metrology institutes when these are applied to the same model of a pressure balance. A comparison with experimental data such as dependence of the effective area on jacket pressure for assemblies operating in the controlled clearance mode, difference between pressure distortion coefficients of two assemblies determined in a cross-float experiment, and, finally, piston fall rates (v_f) has shown significant differences indicating that not all properties of the assemblies analyzed have been adequately taken into account. A sensitivity analysis shows that a profile of the undistorted piston-cylinder clearance, which usually is assumed constant but in reality is not, the boundary conditions on the outer cylinder surface dealing with a behavior of sealing O-rings and the elastic properties of piston-cylinder materials are the main factors influencing the result of numerical modeling. The progress in dimensional metrology currently allows the shape of the piston and cylinder bore to be determined and the data to be incorporated into the model [2]. The stresses caused by the O-rings when a jacket pressure (p_j) is applied can be analyzed and appropriately taken into account [3]. The elastic properties of tungsten carbide materials, which high pressure

piston-cylinders are usually made of, can be directly measured on the piston [4] but not always on the cylinder if the latter is constructed from more than one material. In such cases, since the elastic properties of tungsten carbide hard alloys can vary over a broad range, the elastic distortion of the cylinder becomes the main contribution to the uncertainty budget for the pressure distortion coefficient.

An alternative to the numerical methods is offered by so-called experimental methods which allow the pressure distortion coefficient to be derived from experimentally determined dependencies of piston fall rate and, in the case of assemblies operating in the controlled clearance mode, of the effective area on the jacket pressure. Although these methods are called experimental, in order to get a value of λ from the experimental data, specific models are required and a series of simplifications and assumptions should be made which are valid only to a limited extent. Performance of two different models, one developed by Dadson et al. [5] and the other by Heydemann and Welch [6], applied to a 1 GPa controlled clearance assembly has been analyzed by Schmidt et al. [7]. The former utilizes experimental piston fall rates and must know the pressure distributions in the piston-cylinder interspace. A gap profile used in the hydrodynamic calculation is found assuming that piston and cylinder radial distortions are linear functions of the local pressure in the gap, the line pressure acting on the piston base and the jacket pressure stressing the cylinder from outside. Proportionality coefficients can be determined from elastic constants of the material and piston-cylinder dimensions using Lamé equations or can be adjusted by a fit of the experimental fall rates. This model has been shown not to work adequately as it leads to negative gap widths at pressures at which the assembly operates well. The Heydemann-Welch model uses experimental dependencies of the effective area on jacket pressure and, as an additional parameter, involves a critical jacket pressure at which the cylinder bore surface would touch the piston. This critical jacket pressure cannot be directly determined by experiment without the risk of damaging the assembly and, therefore, is found by extrapolating the cubic root of the piston fall rate to zero over a broad range of the jacket pressure. The uncertainty of this approach and the inappropriateness of the model which is reflected by systematic differences between the experimental and model effective areas and fall rates of a pressure balance studied in [7] at pressures up to 700 MPa have led to the conclusion that neither the Heydemann-Welch nor the Dadson method allow the effective area to be determined with a relative uncertainty smaller than $1.2 \cdot 10^{-4}$, which is equivalent to an uncertainty of $0.17 \cdot 10^{-6}$ MPa^{-1} of the pressure distortion coefficient.

The third experimental method developed by Legras et al. [8] combines features of the two first ones and has been applied at BNM-LNE to characterize primary pressure balances for the 200 MPa pressure range. In this method, the pressure dependent effective area is calculated from a change of the effective area caused by a variation of the jacket pressure from p_{j1} to p_{j2} and the piston fall rates measured at the first and second jacket pressures. The pressure distribution in the piston-cylinder clearance, which should be known for both jacket pressures, is searched assuming the profile of the distorted gap to be a linear or a quadratic function of the axial coordinate with coefficients at which the calculated piston fall rates are equal to the experimental ones. Compared with the original flow method by Dadson et al. [5], which implies use of one cylinder and two pistons of slightly different diameters to change the piston-cylinder gap width, the present method is more effective since the variation of the interspace between piston and cylinder here is easily realized by variation of the jacket pressure. In addition, the problem of a collapsing gap at

high pressures, which is predicted by the Lamé equations, does not occur here because the gap profile determined at each pressure is in agreement with the experimental fall rate. Compared with the Heydemann-Welch method, this approach has an important advantage as it does not require the rather uncertain extrapolation of the fall rate dependencies on jacket pressure down to zero. As was recently reported by Legras [9], the standard deviation of pressure distortion coefficients of five nominally identical assemblies of the BNM-LNE for pressure measurement up to 200 MPa determined by this experimental method is equal to $0.06 \cdot 10^{-6}$ MPa^{-1}; the consistency of the pressure distortion coefficients of each pair of the assemblies checked in cross-float experiments even lies within $0.01 \cdot 10^{-6}$ MPa^{-1}. At the same time the results presented in [9] show that $A_p(p_0 = 200 \text{ MPa}, p_j = 0)$ evaluated from the experimental data measured at p_{j1} and p_{j2} changes in relative terms within $\pm 4 \cdot 10^{-5}$ when different pairs p_{j1} and p_{j2} are taken, which is equivalent to a change of λ within $\pm 0.2 \cdot 10^{-6}$ MPa^{-1}. Neither can this model thus perfectly describe experimental data over the whole range of jacket pressure, so special evaluation procedures to determine λ with a sufficient accuracy are required. This fact and also numerous assumptions made in the method make it very difficult to estimate its uncertainty. In the following, the effect of the assumptions is analyzed and the method is modified to more completely take into account experimental data and to extend it to non-cylindrical piston-cylinder assemblies.

2 Theory

According to Legras et al. [8], the effective area of a controlled clearance piston-cylinder assembly at pressure p_0 and jacket pressure $p_j = 0$, A_{p0}, is

$$A_{p0} = \pi r_0^2 \left[1 + \frac{3\mu - 1}{E} p_0 + \frac{n\left(p_{j2} - p_{j1}\right)}{1 - \left(v_{f2}/v_{f1}\right)^{1/3} I_2/I_1} \right] \tag{1}$$

where r_0 is the radius of the undistorted piston; E and μ are the Young modulus and the Poisson ratio of the piston material, respectively; n is the jacket pressure distortion coefficient, $n = -\partial A_p/\partial p_j \,/\, A_{p0}$; and p_{j1} and p_{j1} are two jacket pressures at which piston fall rates v_{f1} and v_{f2} are measured. I_1 and I_2 denote integrals

$$I = -\int_0^{p_0} \left(\eta \frac{\mathrm{d}x}{\mathrm{d}p} \right)^{1/3} \mathrm{d}p \tag{2}$$

calculated on the basis of fall rates v_{f1} and v_{f2}, respectively, where x is the axial coordinate and $p = p(x)$ a pressure distribution in the gap. To obtain these formulae, the following assumptions have to be made:

(1) Piston and cylinder bore are perfectly cylindrical. Their radii are derived from cross-float and fall rate measurements carried out at sufficiently low pressures at which elastic distortions of piston and cylinder are negligibly small.
(2) The radial distortion of the piston obeys the Lamé equations and is independent of the jacket pressure.
(3) The pressure-transmitting medium is incompressible.

To define the pressure distribution $p(x)$ from the fall rate only, additional assumptions concerning the shape of the clearance between distorted piston and cylinder must be made:

(4) The radial distortion of the cylinder at the gap inlet, $x = 0$, complies with the Lamé equations and allows the gap width there, h_0, to be calculated.

(5) The gap width h_p is a linear or quadratic function of the axial coordinate,

$$h_p = h_0[1+x/l\,(h_l/h_0-1)] \qquad \text{or} \qquad h_p = h_0[1+x^2/l^2\cdot(h_l/h_0-1)],$$

where l is the gap length, and, thus, is unambiguously defined by the gap width at the outlet, $h_l = h_p(l)$, which is adjusted to meet the experimental piston fall rate.

Although both functions are chosen rather arbitrarily and do not necessarily describe a real gap profile, their use is justified by the argument that the errors caused by the choice of the function are eliminated when calculating the ratio of the integrals in Eq. 1. However, from the results presented in [9], it can be concluded that a change from the linear to the quadratic function reduces λ by about $0.3\cdot10^{-6}$ MPa^{-1}.

Let us derive a formula for the effective area without assumptions (1) to (5).

Following Dadson et al. [5], the effective area of an axially symmetrical non-cylindrical piston-cylinder assembly subject to measured and jacket pressures can be expressed as a function of shape deviations of the distorted piston and cylinder and the pressure distribution in the clearance of the assembly:

$$A_p = \pi r^2(0)\left\{1+\frac{R(0)-r(0)}{r(0)}-\frac{1}{r(0)p_0}\int_0^l [r(x)-r(0)+R(x)-R(0)]\frac{\mathrm{d}p}{\mathrm{d}x}\mathrm{d}x\right\}, \tag{3}$$

where $r(x)$ and $R(x)$ are the radii of the non-cylindrical distorted piston and cylinder, respectively. With r_0 denoting the radius of the undistorted piston at $x = 0$, d and u – the radial distortion and shape deviation of the piston, respectively, Eq. 3 can be rewritten as

$$A_p = \pi r_0^2\left[1+\frac{1}{r_0}\bar{h}+D_\mathrm{p}+S_\mathrm{p}\right], \tag{4}$$

where

$D_\mathrm{p} = -\dfrac{2}{r_0 p_0}\displaystyle\int_0^l d\,\frac{\mathrm{d}p}{\mathrm{d}x}\mathrm{d}x$ is the piston distortion contribution,

$S_\mathrm{p} = -\dfrac{2}{r_0 p_0}\displaystyle\int_0^l u\,\frac{\mathrm{d}p}{\mathrm{d}x}\mathrm{d}x$ is the piston shape contribution,

$\dfrac{\bar{h}}{r_0} = -\dfrac{1}{r_0 p_0}\displaystyle\int_0^l h_p\,\frac{\mathrm{d}p}{\mathrm{d}x}\mathrm{d}x = \frac{1}{r_0 p_0}\int_0^{p_0} h_p\mathrm{d}p$ is the gap contribution.

Using the relation between the volumetric fluid flow through the piston-cylinder gap and the piston fall rate,

$$-\frac{\pi r_0 h_p^3}{6\eta(p)}\frac{\mathrm{d}p}{\mathrm{d}x} = \pi r_0^2 v_\mathrm{f}\frac{\rho(p_0)}{\rho(p)},$$

where η and ρ are the pressure dependent viscosity and density of the fluid, the gap contribution to the effective area can be defined as

$$\frac{\bar{h}}{r_0} = VI, \quad \text{where} \quad V = \frac{(6r_0\rho_0 v_\mathrm{f})^{1/3}}{r_0 p_0} \quad \text{and} \quad I = \int_0^l\left(\frac{\eta}{\rho}\right)^{1/3}\left(-\frac{\mathrm{d}p}{\mathrm{d}x}\right)^{2/3}\mathrm{d}x = \int_0^{p_0}\left(-\frac{\eta}{\rho}\frac{\mathrm{d}x}{\mathrm{d}p}\right)^{1/3}\mathrm{d}p\,. \tag{5}$$

Differentiating the left and right sides of Eq. 4 over p_j,

$$\frac{\partial A_p}{\partial p_\mathrm{j}} \equiv -A_{p0} n = \pi r_0^2 \left[\frac{1}{r_0} \bar{h}' + D_\mathrm{p}' + S_\mathrm{p}' \right],$$

where the symbols with an apostrophe designate derivatives $\partial\ldots/\partial \mathrm{p_j}$, defining $\bar{h}'/r_0$ in three different ways

$$\frac{1}{r_0}\bar{h}' = VI' + V'I = \begin{cases} \dfrac{\bar{h}}{r_0}\dfrac{I'}{I} + V'I \\ \dfrac{\bar{h}}{r_0}\dfrac{V'}{V} + I'V \\ \dfrac{\bar{h}}{r_0}\left(\dfrac{V'}{V} + \dfrac{I'}{I}\right) \end{cases}, \tag{6}$$

expressing then $\bar{h}/r_0$ over $\bar{h}'/r_0$ and substituting it into Eq. 4, three equations for A_{p0} can be obtained:

$$A_{p0} = \pi r_0^2 \frac{1 + D_\mathrm{p} + S_\mathrm{p} - \left(IV' - D_\mathrm{p}' - S_\mathrm{p}'\right) I/I'}{1 - n\left(p_\mathrm{j} - I/I'\right)}, \tag{7}$$

$$A_{p0} = \pi r_0^2 \left[1 + D_\mathrm{p} + S_\mathrm{p} + n\left(p_\mathrm{j} - \frac{V}{V'} \right) - (D_\mathrm{p}' + S_\mathrm{p}' + I'V)\frac{V}{V'} \right], \tag{8}$$

$$A_{p0} = \pi r_0^2 \left[1 + D_\mathrm{p} + S_\mathrm{p} + n\left(p_\mathrm{j} - \frac{1}{V'/V + I'/I} \right) - \frac{D_\mathrm{p}' + S_\mathrm{p}'}{V'/V + I'/I} \right], \tag{9}$$

in which the terms of an order higher than h_0/r_0 are omitted. It can be shown that, among of the three equations obtained, it is Eq. 9 which turns into Eq. 1 of Legras et al. [8] if the piston and cylinder bore are taken as cylindrical ($S_\mathrm{p} = 0$, $S_\mathrm{p}' = 0$), the piston contribution is calculated according to Lamé ($D_\mathrm{p} = (3\mu\text{-}1)p_0/E$) and is independent of jacket pressure ($D_\mathrm{p}' = 0$), and the derivatives V' and I' are replaced by $(V_2\text{-}V_1)/(p_{\mathrm{j}2}\text{-}p_{\mathrm{j}1})$ and $(I_2\text{-}I_1)/(p_{\mathrm{j}2}\text{-}p_{\mathrm{j}1})$, respectively.

In Eqs. 7-9, r_0, n, V and V' are experimental quantities and S_p, D_p and I are calculated as functions of the jacket pressure and are then differentiated by p_j to find S_p', D_p' and I'. Whereas S_p, D_p are unequivocal, the pressure distribution in the piston-cylinder gap required for the calculation of I can be determined differently. Three methods to calculate $p(x)$, which seemed to be the most reliable ones, were investigated in this work.

The first one is an iterative approach described e.g. in [2] in which a calculation of the distorted gap profile using the FEA, $h_{p,\mathrm{FEA}}$, and a calculation of the pressure distribution in the gap using the model of a one-dimensional viscous flow, $p_{\mathrm{FEA}}(x)$, are carried out alternately till convergence is obtained. Basically, this method of $p_{\mathrm{FEA}}(x)$ determination is equivalent to the Dadson approach [5] but has as an important advantage that the gap does not close where the pressure in the gap becomes low. The piston fall rates corresponding to the calculated pressure distribution can conflict with the experimental ones.

In the second method, the gap profile obtained by the first method, $h_{p,\mathrm{FEA}}$, is additionally corrected to $h^*_{p,\mathrm{FEA}}$ according to

$$h^*_{p,\mathrm{FEA}} = h_{p,\mathrm{FEA}} + \Delta h_l \left[1 - \left(1 - \frac{x}{l} \right)^{1/2} \right], \tag{10}$$

where parameter Δh_l is the gap width correction at the outlet and is searched to obtain the experimental piston fall rate, and then a corrected pressure distribution, $p^*_{\mathrm{FEA}}(x)$, is calculated. The choice of the function in Eq. 10 is based on the observation that a gap between distorted piston and cylinder usually is of parabolic shape, with a rapid change of the width and the highest curvature of the profile at the gap outlet. It should be noted that the correction in Eq. 10 is substantially smaller than h_p so that h_p^* mostly describes the real gap profile plus distortions furnished by the FEA.

In the third method, both V and I are determined from $p_{\mathrm{FEA}}(x)$ and $h_{p,\mathrm{FEA}}$ calculated by the FEA. Thus, this method differs from method 1 by the use of the FEA-calculated fall rate instead of the experimental one. In fact, this variant of the experimental method is closest to the FEA method because all quantities are calculated and only the jacket pressure distortion coefficient is experimental.

In the next but one section, these three methods and the performance of Eqs. 7-9 are tested when applied to a 1 GPa piston-cylinder assembly which was investigated in detail by experiment and by means of the FEA.

3 Experimental and FEA results

The piston-cylinder assembly under study is a 1 GPa assembly of 5 mm^2 nominal effective area manufactured produced by Desgranges et Huot (DH), France, and has the serial number 7594. Normally, piston-cylinders of this type are used as a high pressure assembly in a DH commercial 1:10 multiplier whose construction has been described in detail by Delajoud [10]. The assembly is one of the three units of this type available at PTB and used for the realization of the pressure scale in the pressure range up to 1 GPa. It is mounted in a modified Harwood twin pressure balance where it can be loaded with a maximum weight of 500 kg and is operated in the controlled clearance mode at a jacket pressure equal to 10 % of the measured pressure [11]. The equipment allows also experiments with varying jacket pressure to be performed. Typical relative standard deviations of the zero-pressure effective area obtained from cross-float experiments are $3 \cdot 10^{-6}$ when comparing with the Ruska 8.4 mm^2 assemblies operating at pressures up to 400 MPa, and $6 \cdot 10^{-6}$ when cross-floating against other 1 GPa units of the same type over the entire pressure range of 1 GPa.

The results of piston fall rate and effective area measurements at variable jacket pressure are presented in Figs. 1 and 2. The cubic roots of the experimental fall rates vs. jacket pressure are not absolutely linear and require polynomials of the second degree to be well fitted. If these dependencies were used to determine the effective area by the Heydemann-Welch method, significant errors might occur when extrapolating the experimental data to zero fall rates. In contrast to the fall rates, the dependencies of the effective area on jacket pressure do not show any systematic deviation from a linear law and allow n to be determined with the combined standard uncertainties, $u(n)$, given in Table 1.

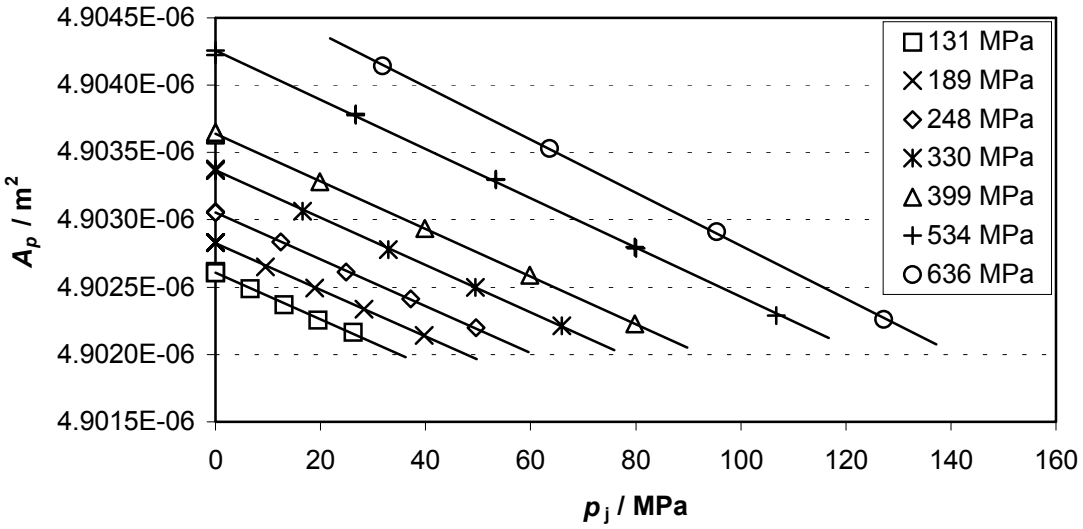

Figure 1. Effective area vs. jacket pressure at different p_0

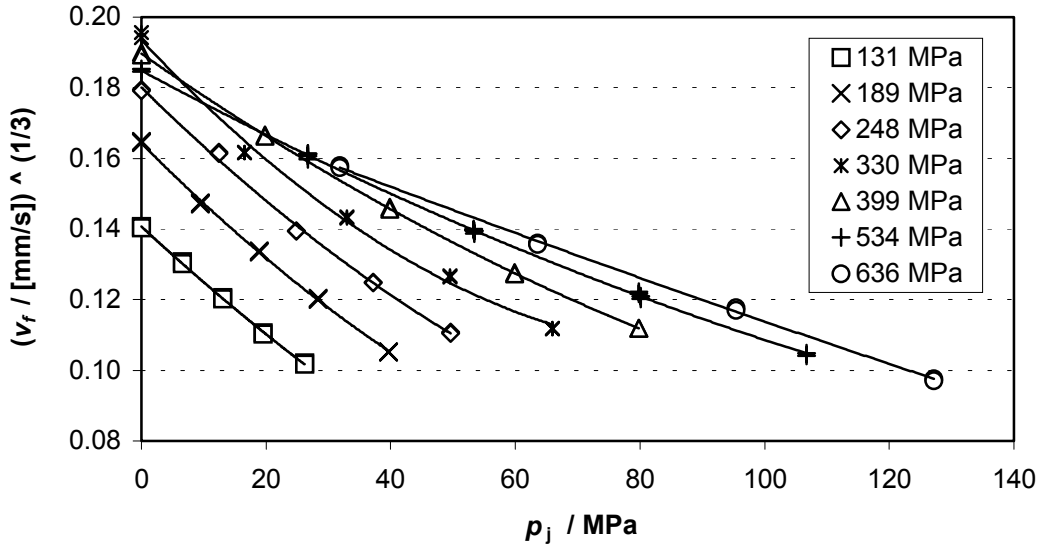

Figure 2. (Piston fall rate)$^{1/3}$ vs. jacket pressure at different p_0 fitted by polynomials of second order

The jacket pressure distortion coefficient was also determined by calibration of the assembly in the free deformation and controlled clearance operation modes in a pressure range of (40-400) MPa using a Ruska 400 MPa assembly as a standard. From the pressure distortion coefficients in these two operation modes, λ_{FD} and λ_{CC}, n with its standard uncertainty was found to be

$$n = p_0/p_j\,(\lambda_{FD}\text{-}\lambda_{CC}) = (3.39\pm0.18)\cdot10^{-6}\ \text{MPa}^{-1}$$

and thus agrees with the values obtained by the direct n measurements within the sum of the uncertainties of the two results.

Table 1. Experimental jacket pressure distortion coefficients

p_0 / MPa	n / (10^{-6} MPa^{-1})	$u(n)$ / (10^{-6} MPa^{-1})
131	3.55	0.24
189	3.55	0.11
248	3.55	0.09
330	3.59	0.08
399	3.61	0.06
534	3.72	0.13
636	4.02	0.12

The pressure distortion coefficients of the assembly were calculated applying the FEA. A drawing of the cylinder and a model of the assembly used in the FEA are shown in Fig. 3.

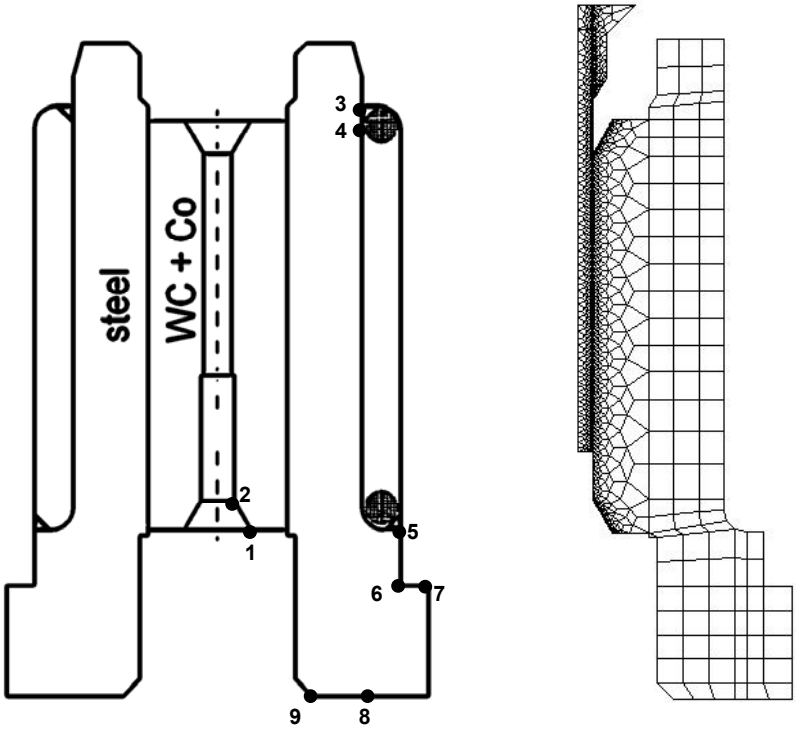

Figure 3. Design of the cylinder (left) and the model of assembly used in FEA

In the analysis, section 4-5 was loaded with the jacket pressure and sections 6-7, 8-9 and 1-2 were constrained. Alternatively, section 3-4 was also subjected to p_j and section 1-2, which touches a pressure-transmitting tube, was subjected to p_0, to study the effect of the boundary conditions. The piston and cylinder surfaces below the entrance to the gap were loaded with p_0, and their surfaces along the coupling length were loaded with a pressure distribution obtained by hydrodynamic calculation. This was performed taking into account the pressure dependent density and viscosity of di(2-ethylhexyl) sebacate, which is used in the pressure balance as a working fluid, whose values were taken from the work by Vergne [12] and the report [13]. The gap between undistorted piston and cylinder was on the one hand considered to be constant with a width (0.32±0.03) μm as obtained from piston fall rate measurements at low pressures and on

the other hand it was measured at the Geometrical Standards Section of the PTB (Fig. 4). In the analysis, an axially symmetrical model was used and the half diameters measured at the same height for different angular directions were averaged.

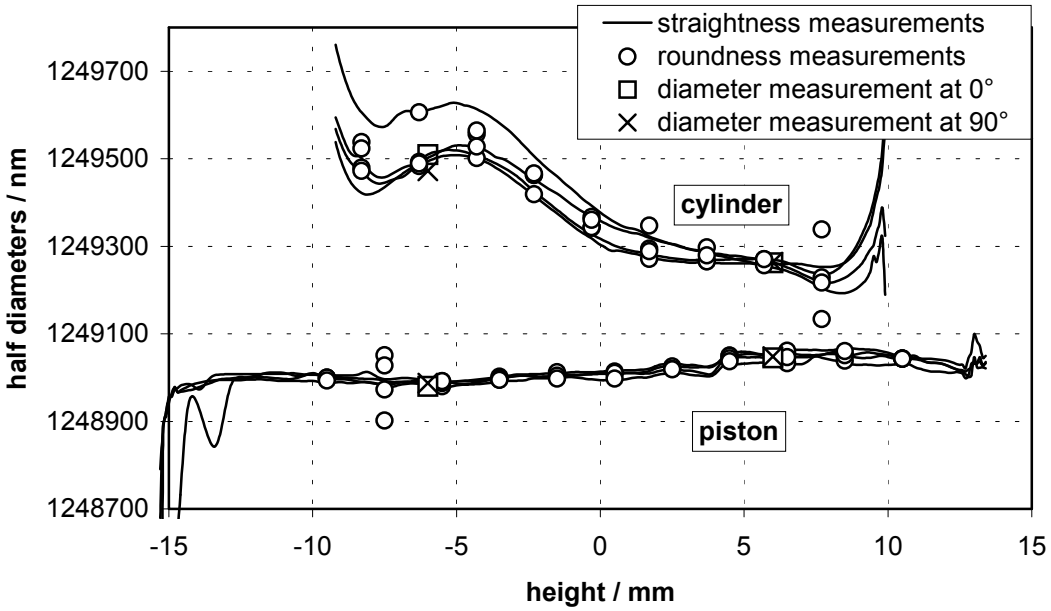

Figure 4 Half diameters of piston and cylinder of unit DH 7594 measured in different azimuthal directions

The elastic properties of the cylinder steel sleeve surrounding the core of tungsten carbide (WC) are E_{st} = (200±7) GPa and μ_{st} = 0.29±0.02. According to information from Desgranges et Huot, the elastic constants of the hard alloy the assembly is made of are $E_{WC,DH}$ = 630 GPa and $\mu_{WC,DH}$ = 0.22. As the uncertainty of these values was unknown and the material identical with that of the assembly was not available, the elastic constants were measured directly on the piston using strain gauges [4] with the results $E_{WC,PTB}$ = (543±7) GPa and $\mu_{WC,PTB}$ = (0.238±0.002). Due to the construction of the cylinder, application of this method to the cylinder WC core is not possible. For this reason, tangential strain measurements were carried out on the cylinder steel part when the assembly was operating in the free deformation mode. The measured strains were compared with those calculated at the same places using FEA, once assuming the elastic properties of the WC core to be as measured at PTB on the piston, and once using the values reported by Desgranges et Huot. A comparison has shown that the cylinder properties should be close to the DH values rather than to the PTB values. Finally, the cylinder core material was concluded to be different from that of the piston and to have elastic constants lying somewhere between the DH and PTB values. With the two different materials of the cylinder core, FEA yields two pressure distortion coefficients which differ by:

$$\Delta_{E,\mu}(\lambda_{CC}) = \lambda_{CC,\ \text{cyl. } E,\mu = \text{pst. } E,\mu} - \lambda_{CC,\ \text{cyl. } E,\mu \text{ from DH}} = 0.12 \cdot 10^{-6}\ \text{MPa}^{-1}.$$

The use of the constant and real shape gaps between the undistorted piston and cylinder results in two distortion coefficients which differ by:

$$\Delta_{gap}(\lambda_{CC}) = \lambda_{CC,\ \text{const. gap}} - \lambda_{CC,\ \text{real gap}} = -0.09 \cdot 10^{-6}\ \text{MPa}^{-1}.$$

Compared with other uncertainty sources which altogether lead to a combined standard uncertainty $u(\lambda_{CC}) = 0.013 \cdot 10^{-6}$ MPa^{-1}, the elastic properties of the WC cylinder are clearly the main contributions to the uncertainty of λ_{CC}. The FEA results for two different gaps demonstrates that the pressure distortion coefficient can significantly deviate from a correct value if a non-cylindrical assembly is treated as a cylindrical one. The results presented in Fig. 5 show that none of the models used in the FEA can perfectly reproduce the experimental dependence of n on p_0.

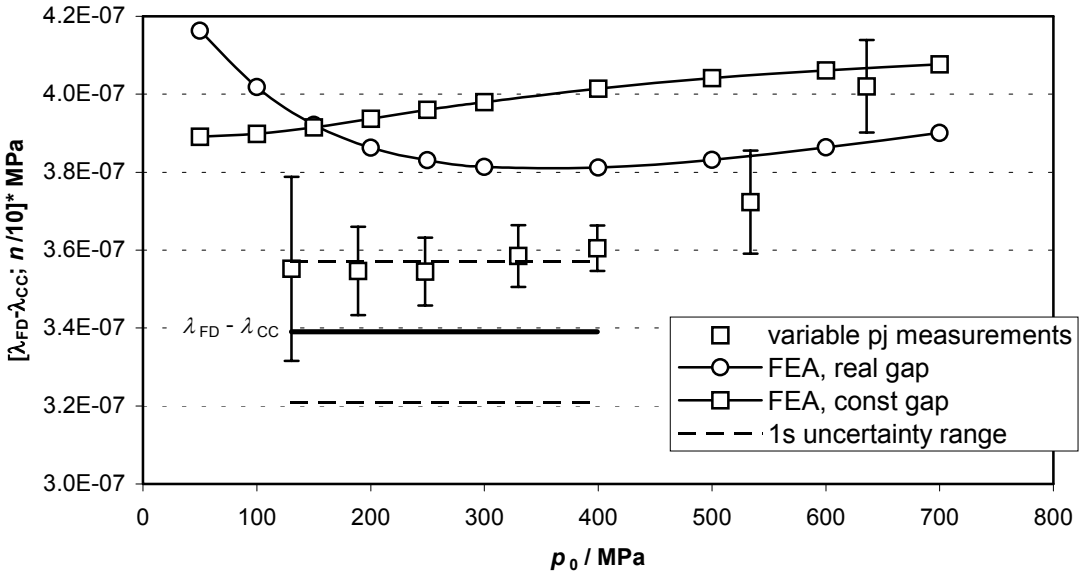

Figure 5. $1/10^{th}$ of jacket pressure distortion coefficient vs. pressure

Results by modified experimental method

Initially, to study the performance of the three Eqs. 7-9, all the terms including n and V, which usually are obtained from an experiment, were calculated using FEA.

The contribution of the piston distortion to the effective area is practically independent of the jacket pressure – D_p changes only by 10^{-8} at $p_0 = 330$ MPa and by $5 \cdot 10^{-7}$ at $p_0 = 636$ MPa when p_j varies in the range (0 to 0.2)p_0. The differences between the values calculated by the FEA and the Lamé equation are even smaller than the D_p-variations. Thus, the assumption concerning the piston distortion law is absolutely correct.

To find the derivatives V', S_p' and I', the jacket pressure dependencies of V, S_p and I were fitted by polynomials of appropriate order and then differentiated. As was shown in the previous section, a description of $v_f^{1/3}(p_j)$ by polynomials of second order is sufficient. Dependencies $S_p(p_j)$ given in Fig. 6 for two p_0 show that a quadratic or even linear fit is enough. In dependence on p_0 and p_j, S_p supplies a contribution of $(0.08 \text{ to } 0.2) \cdot 10^{-6}$ MPa^{-1} to the pressure distortion coefficient and, therefore, would lead to a significant error, if the piston were treated as cylindrical.

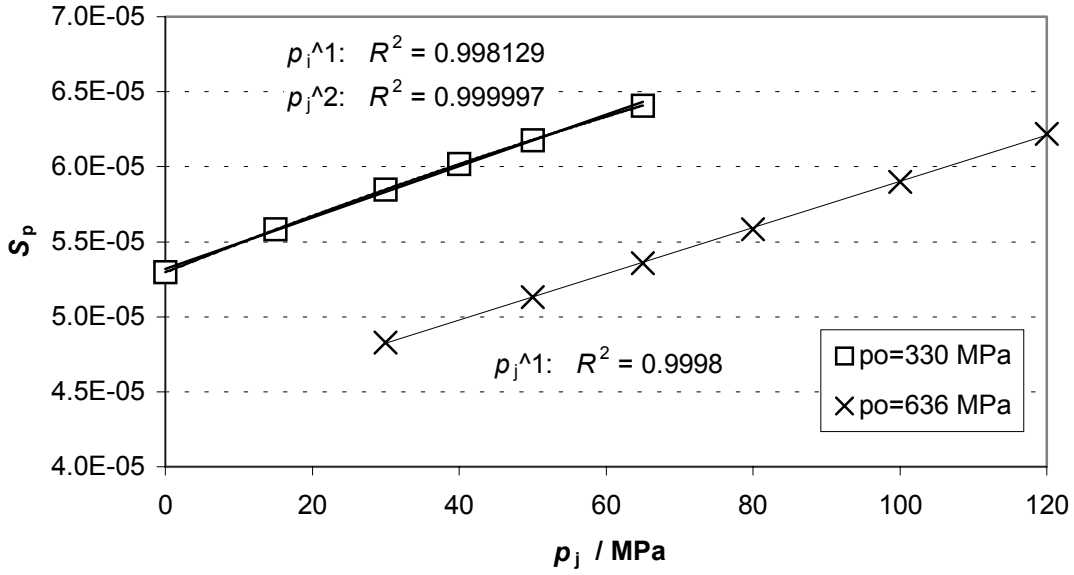

Figure 6. Piston shape contribution to the effective area. R^2 – squared correlation coefficient for fits of 1st (p_j^1) and 2nd (p_j^2) order

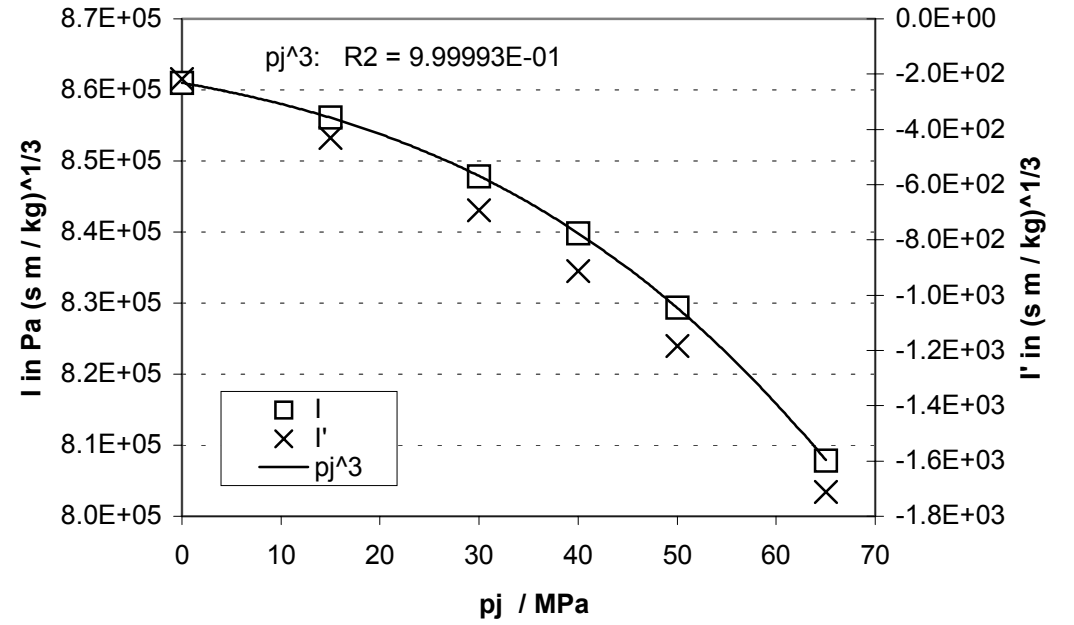

Figure 7. I and I' at p_0 = 330 MPa

To describe $I(p_j)$, a polynomial at least of third order is required (Fig. 7). While I changes only by about 5 %, its derivative I' varies by a factor of 20. The ratio I/I' spreads from 4000 MPa at p_j=0 MPa to 500 MPa at p_j=65 MPa and is much higher than p_j. For this reason, the uncertainty of I is expected to play an important role especially in Eq. 7, which contains the difference $(p_j - I/I')$, and particularly at lower jacket pressures. In Eq. 8, term $n(p_j - V/V')$ appears instead of $n(p_j - I/I')$. An uncertain V has a smaller effect on A_{p0} than an uncertain I because V/V' is nearly

constant and has the order of p_j when the latter approaches $0.2p_0$. However, here too, a lower accuracy of the method is expected at lower jacket pressures at which the ratio between p_j and V/V' becomes unfavorable. The effect of uncertain I' in the last brackets in Eq. 8 is moderate because $I'V$ is everywhere smaller than n by a factor 4. In Eq. 9, I'/I is significantly smaller than V'/V at low jacket pressures and reaches $\approx 0.3V'/V$ at $p_j=0.2p_0$. As a result, $1/(V'/V + I'/I) \approx V/V'$ so that the reasoning applied to Eq. 8 is also valid for Eq. 9. This analysis allows the conclusion to be drawn that the experimental method should furnish more reliable results at higher jacket pressures, which will be supported later by the results based on the experimental data.

Following this conclusion, v_f and n values should be measured at as high jacket pressures as possible. Since a maximum jacket pressure in an experiment is restricted for several reasons, one could try to extrapolate V'/V and I'/I to jacket pressures over the range in which measurements are not possible. When the jacket pressure reaches a critical value at which v_f becomes zero, uncertainties of V and I no longer have an effect on A_{p0} because term $1/(V'/V + I'/I)$ in Eq. 9 tends to zero. It can easily be seen that under such conditions the actual experimental method changes into the Heydemann-Welch method [6].

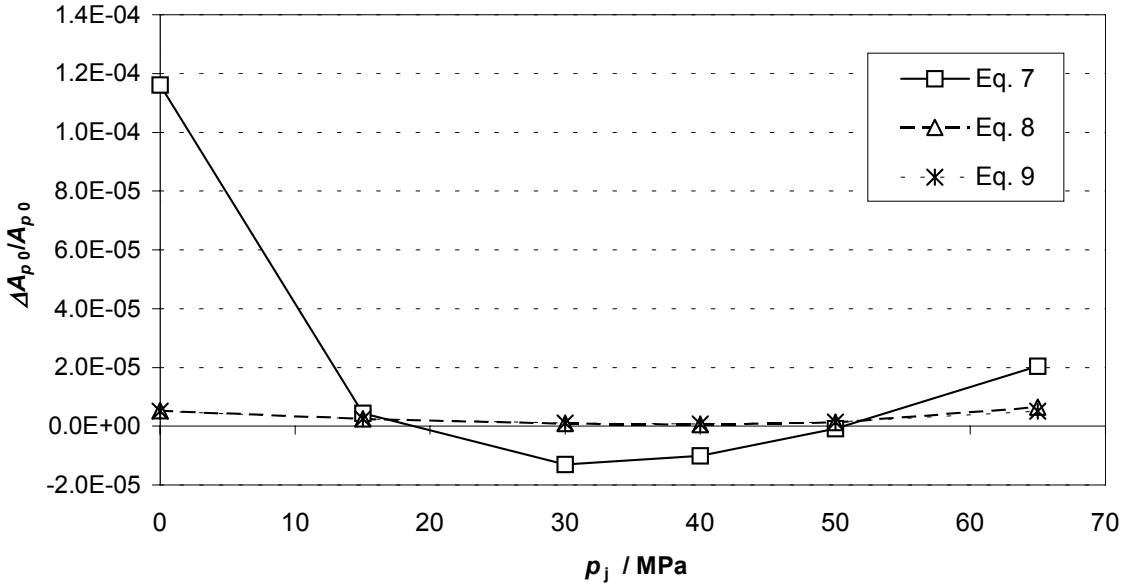

Figure 8. Relative deviations of A_{p0} calculated by Eqs. 7-9 from A_{p0} calculated by FEA at p_0 = 330 MPa

The results of the test A_{p0} – calculation in which all required quantities are obtained from FEA demonstrate that Eqs. 8 and 9 work better than Eq. 7 and yield the smallest deviation from the effective area directly calculated by FEA at p_j = 0 (Fig. 8). The values obtained by Eqs. 8 and 9 are almost the same and deviate from the FEA values by less than $5 \cdot 10^{-6}$ in relative terms. In the following analysis, only Eqs. 8 and 9 are used.

The dependence of A_{p0} on p_0 as obtained for five jacket pressures by the modified experimental method referred to as method 1 (n, v_f –experimental, $p(x)$ – FEA-calculated) is presented together with an FEA-based dependence in Fig. 9. As a reference effective area A_0, the value calculated from the dimensional data for the piston-cylinder bore was taken. This value was higher than the

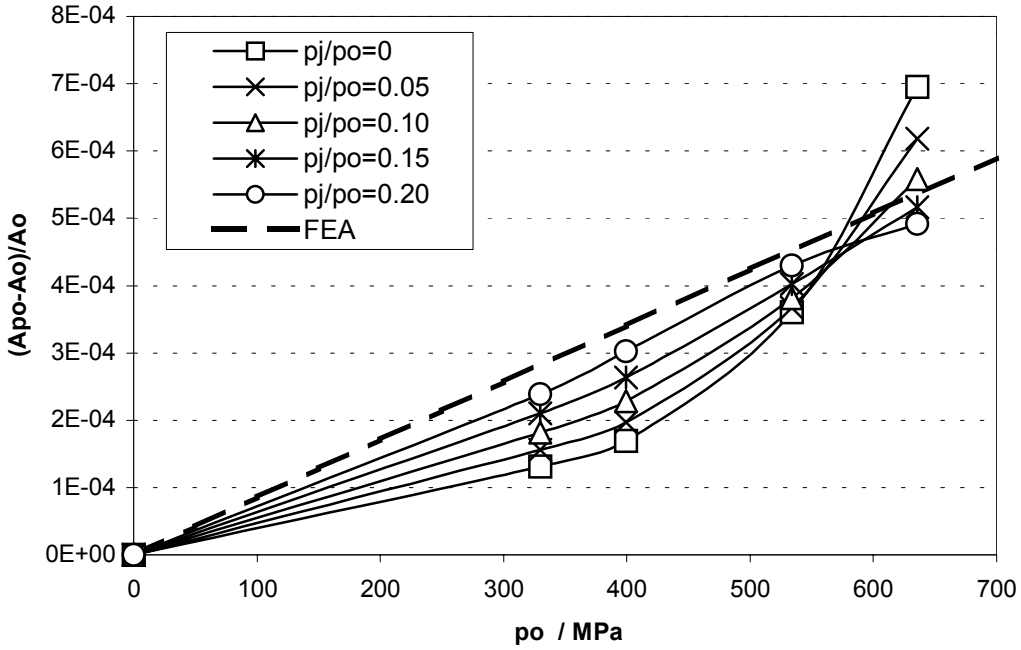

Figure 9. Relative change of the effective area determined by the FEA and modified experimental method 1

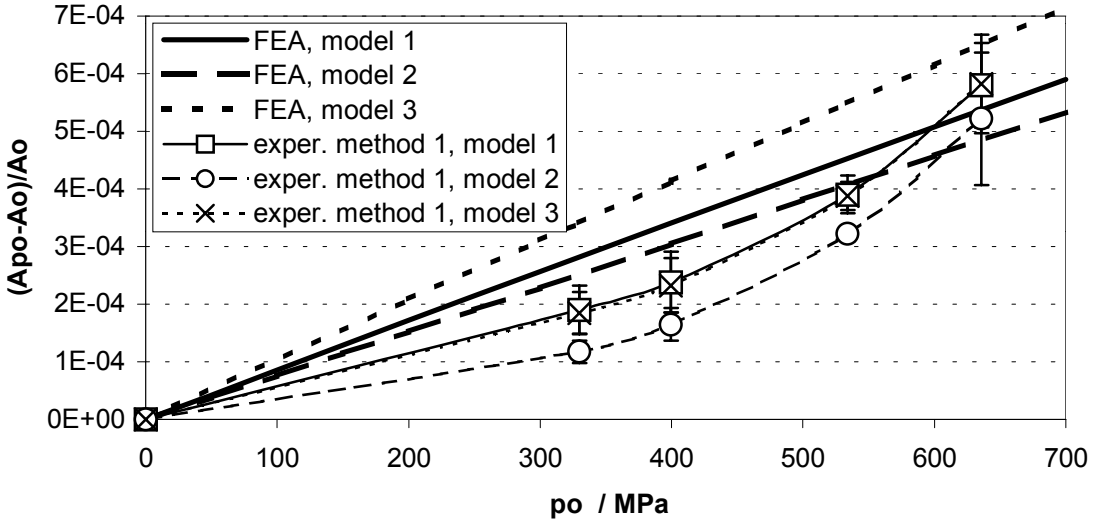

Figure 10. Effect of elastic constants of the cylinder and of the profile of undistorted gap on the pressure dependent effective area determined by the FEA and experimental method 1: model 1 – real gap, E = 630 GPa, μ = 0.22; model 2 – const. gap, E = 630 GPa, μ = 0.22; model 3 – real gap, E = 543 GPa, μ = 0.238. Points are non-weighted means at each p_0, vertical bars show their standard deviations.

effective area determined from the cross-float experiments by only $7 \cdot 10^{-6}$ in relative units. The systematic deviation from a linear law, which is particularly strong at low jacket pressures, is due to method inconsistency. The dependence obtained using the highest jacket pressure $p_j = 0.2p_0$ is the most linear one and close to the FEA results.

Figure 10 shows how the elastic constants of the cylinder and the piston-cylinder gap geometry affect the pressure dependent effective area determined by the FEA and the experimental method. The results furnished by experimental method 1 are almost insensitive to the elastic properties of the cylinder but strongly depend on the initial gap shape.

To obtain the pressure distortion coefficient from the experimental data shown in Fig. 9, three fitting procedures were tested:

A_0 – experimental; λ_{FD} – fitted:
$$\sum_{p_0}\sum_{p_j}\left[A_{p0}(p_0,p_j) - A_0(1+\lambda_{FD}p_0)\right]^2 \rightarrow \min \qquad (11)$$

A_0 – experimental; λ_{FD} – fitted:
$$\sum_{p_0}\sum_{p_j}\left[A_{p0}(p_0,p_j) - A_0(1+\lambda_{FD}p_0)\right]^2 (p_j/p_0)^2 \rightarrow \min \qquad (12)$$

A_0 and λ_{FD} – fitted:
$$\sum_{p_0}\sum_{p_j}\left[A_{p0}(p_0,p_j) - A_0(1+\lambda_{FD}p_0)\right]^2 (p_j/p_0)^2 \rightarrow \min \qquad (13)$$

In Eq. 11, all experimental values are taken with the same weight, whereas in Eq. 12, they are weighted by p_j according to the conclusion drown before as regards the better performance of the experimental method at higher jacket pressures. The values of λ_{FD} obtained by Eqs. 11 and 12 are very close, but the standard deviations furnished by the non-weighted fit are significantly greater. All λ_{FD} obtained by Eq. 13 are systematically greater than those from Eqs. 11 and 12 by about $(0.06 \text{ to } 0.15) \cdot 10^{-6}$ MPa^{-1}, have standard deviations of $(0.08 \text{ to } 0.15) \cdot 10^{-6}$ MPa^{-1} and thus statistically agree with the results from Eqs. 11 and 12. Nevertheless, Eq. 13 has an important advantage over Eqs. 11 and 12, as it furnishes results which do not depend on A_0 and consequently are less sensitive to dimensional piston-cylinder properties.

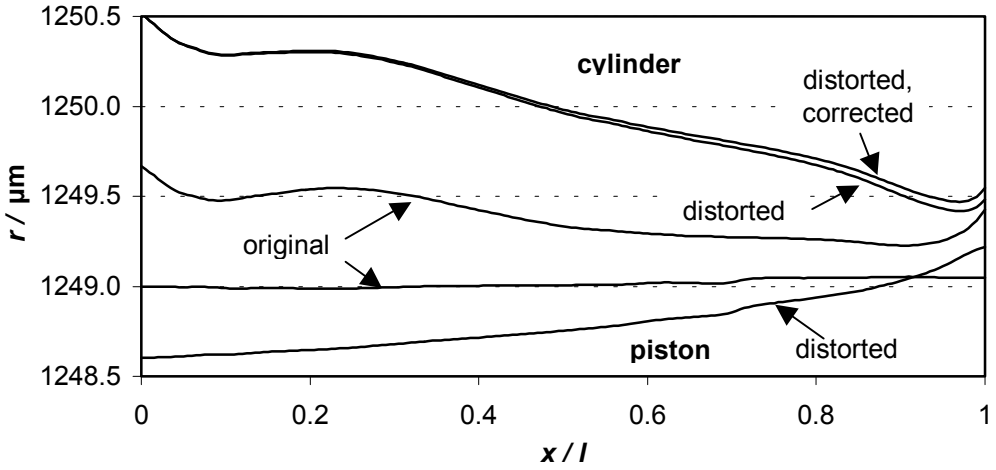

Figure 11. Radii of undistorted and distorted piston and cylinder as well as radii of distorted cylinder corrected by Eq. 10, all determined at $p_0 = 330$ MPa and $p_j = 0$

The difference between the gap profile determined by the FEA and used in method 1, and the gap profile corrected by Eq. 10 and used in method 2 is shown in Fig. 11. The gap correction is much smaller than the gap width calculated by the FEA and, finally, change λ by about $0.05 \cdot 10^{-6}$ MPa^{-1}.

In Table 2, the results obtained by the three variants of the modified experimental method and by the FEA are compiled. The results obtained with the experimental methods are those furnished by a fitting approach to the experimental data according to Eq. 12. All calculations were performed for the elastic constants of the piston as measured at PTB (pst. E,μ) and the elastic constants of the cylinder WC core reported by Desgranges et Huot (E,μ from DH). The uncertainty contributions are: $s(\lambda)$ – standard deviation due to model inconsistency; $u_n(\lambda)$ – standard uncertainty caused by the jacket pressure distortion coefficient in the experimental methods, $u_n(\lambda) = u(\mathrm{n}) \cdot \max\left| p_\mathrm{j} - 1/[V'/V + I'/I] \right|$; $\Delta_{E,\mu}(\lambda) = \lambda_{\text{cyl. } E,\mu = \text{pst. } E,\mu} - \lambda_{\text{cyl. } E,\mu \text{ from DH}}$ – effect of the elastic constants of the cylinder; $\Delta_{\mathrm{gap}}(\lambda) = \lambda_{\text{const. gap}} - \lambda_{\text{real gap}}$ – effect of undistorted gap profile; $\max\left| 0.1n - (\lambda_{\mathrm{FD}} - \lambda_{\mathrm{CC}}) \right|$ - maximum deviation from experimental jacket pressure distortion coefficient.

Table 2. Pressure distortion coefficients and uncertainty contributions in the pressure range (300-700) MPa calculated by the FEA and three modified experimental methods

	FEA	Modified experimental methods		
		Method 1: v_f – experim., I – FEA	Method 2: v_f – experim., I – FEA + correction to meet v_f	Method 3: v_f – FEA, I – FEA
$\lambda_{\mathrm{FD}} \cdot 10^6$ MPa	0.847	0.778	0.836	0.834
$s(\lambda_{\mathrm{FD}}) \cdot 10^6$ MPa	0.004	0.040	0.041	0.021
$u_n(\lambda_{\mathrm{FD}}) \cdot 10^6$ MPa	0	0.06	0.06	0.06
$\Delta_{\mathrm{E},\mu}(\lambda_{\mathrm{FD}}) \cdot 10^6$ MPa	0.18	-0.020	-0.071	-0.092
$\Delta_{\mathrm{gap}}(\lambda_{\mathrm{FD}}) \cdot 10^6$ MPa	-0.08	-0.19 / +0.011 *)	-	-
$\lambda_{\mathrm{CC}} \cdot 10^6$ MPa	0.460	0.397	0.455	0.453
$s(\lambda_{\mathrm{CC}}) \cdot 10^6$ MPa	0.008	0.035	0.036	0.013
$u_n(\lambda_{\mathrm{CC}}) \cdot 10^6$ MPa	0	0.05	0.05	0.05
$\Delta_{\mathrm{E},\mu}(\lambda_{\mathrm{CC}}) \cdot 10^6$ MPa	0.12	-0.020	-0.071	-0.092
$\Delta_{\mathrm{gap}}(\lambda_{\mathrm{CC}}) \cdot 10^6$ MPa	-0.09	-0.20 / +0.011 *)	-	-
$\max\left\|0.1n - (\lambda_{\mathrm{FD}} - \lambda_{\mathrm{CC}})\right\| \cdot 10^6$ MPa	0.027	0	0	0

*) Results obtained by the regression procedure according to Eq. 13

All the pressure distortion coefficients are consistent with one another within their standard uncertainties. One significant uncertainty contribution of the experimental methods deals with the methods themselves – they are not capable of adequately describing experimental n and v_f over entire ranges of p_0 and p_j. The standard deviation would even be greater by a factor of 3.5 if p_j - nonweighted fit (Eq. 11) were used. The main reason for this evidently is the experimental piston fall rate, which, due to possible leak, temperature instability and piston-cylinder eccentricity, is the most unsafe experimental parameter of the method. If the experimental fall

rates are replaced by those calculated by the FEA (method 3), $s(\lambda)$ decreases by the factor 2. All three variants of the experimental method are less sensitive to the elastic properties of the cylinder than the FEA method, for method 1 this dependence is extremely weak. This result reflects that the information which in the FEA method is represented by the two parameters, E and μ, is expressed in the experimental methods by three parameters, E, μ and n, the last of which remains constant while E and μ change. It appears, however, to be unusual that the decrease in the rigidity of the cylinder material, which should increase λ and does so in the FEA case, reduces λ furnished by the experimental methods. An analysis performed for the model of the perfectly cylindrical piston and cylinder by method 1 demonstrates that the experimental method is very sensitive to the information on the gap profile if a fixed value of A_0 is used in the regression procedure (Eqs. 11 and 12). The changes of λ_{FD} and λ_{CC}, which are $-0.19 \cdot 10^{-6}$ MPa^{-1} and $-0.20 \cdot 10^{-6}$ MPa^{-1}, are in conformity with the piston shape effect S_p estimated above and supply up to $0.2 \cdot 10^{-6}$ MPa^{-1} into the pressure distortion coefficient. In contrast to Eqs. 11 and 12, Eq. 13 indicates a change of only $+0.011 \cdot 10^{-6}$ MPa^{-1} in both λ_{FD} and λ_{CC}. A comparison of the uncertainties by the experimental methods shows that, in the sequence from method 1 to method 3, the consistency of the methods improves but the sensitivity to the elastic constants of the cylinder increases. In the experimental methods, all uncertainty contributions with the exception of the gap profile are smaller for λ_{CC} than for λ_{FD}. Finally, the pressure distortion coefficients with their combined standard uncertainties are:

	FEA	**Modified experimental methods**
$[\lambda_{FD} \pm u(\lambda_{FD})] \cdot 10^6$ **MPa =**	**0.847 ± 0.10**	**0.816 ± 0.080**
$[\lambda_{CC} \pm u(\lambda_{CC})] \cdot 10^6$ **MPa =**	**0.460 ± 0.071**	**0.435 ± 0.070**

It should be noted that the uncertainty of the dimensional data of the gap is not included in the uncertainties.

5 Conclusions

The experimental method considered above allows the uncertainty of the pressure distortion coefficient caused by the elastic properties of the cylinder to be reduced compared with the FEA method. Inconsistency of the model, unsafe piston fall rates, uncertainties of the jacket pressure distortion coefficient and arbitrarily calculated pressure distribution in the piston-cylinder interspace are the main uncertainty sources of the method. For the piston-cylinder assembly DH 7594, which is used at PTB for the realization of the pressure scale up to 1 GPa, the pressure distortion coefficients determined by the FEA and the modified experimental method in the pressure range (300 to 700) MPa in the free deformation and controlled clearance operation modes are in good agreement. The uncertainties of the distortion coefficient obtained by these two methods for the controlled clearance mode are practically the same. If the elastic constants of the cylinder were better known, the FEA would furnish smaller uncertainties than the experimental method. Knowledge of the dimensional properties of the piston-cylinder gap is important for the experimental as well as for the FEA method.

Acknowledgements

The author wishes to thank Dr. J. Jäger, head of the PTB Pressure Section for his support for this work. Sincere thanks are directed to Mr. D. Wassmann of the PTB Pressure Section, who performed all the cross-float and piston fall rate measurements. Also, the cooperation of Dr. O. Jusko, head of the PTB Geometrical Standards Section, who managed the measurements of the dimensional piston-cylinder properties is gratefully appreciated.

References

1. G.F. Molinar, W. Sabuga, G. Robinson, and J.C. Legras, Comparison of methods for calculating distortion in pressure balances up to 400 MPa - EUROMET Project #256, *Metrologia*, 1998, vol. 35, pp. 739-759
2. W. Sabuga, Elastic distortion calculations at PTB on a PTB 400 MPa pressure balance as part of EUROMET Project 256, PTB Report W-60, Braunschweig, March 1995
3. W. Sabuga, Elastic distortion calculations at PTB on LNE 200 MPa pressure balances as part of EUROMET Project 256. PTB Report W-63, Braunschweig, November 1995
4. W. Sabuga, Determination of elastic properties of piston gauges using the strain gauge method, in: *Proc. of the 17th International Conference on Force, Mass, Torque and Pressure Measurements*, IMEKO TC3, Istanbul, Turkey, 17-21 Sept. 2001, pp. 380-385
5. R.S. Dadson, R.G.P. Greig, and A. Horner, Developments in the accurate measurement of high pressures, *Metrologia*, 1965, vol. 1, pp. 55-67
6. P.L.M. Heydemann and B.E. Welch, *Experimental thermodynamics*, vol. II, edited by B. LeNeindre and B. Vodar, Butterworth, London, 1975, pp. 147-201
7. J.W. Schmidt, D. Ward, S.A. Tison, Research at high pressure (primary pressure standards), in: *1997 of NCSL Workshop & Symposium*, pp. 183-194
8. J.C. Legras, A. Huot, P. Delajoud, La référence nationale de pression du BNM dans le domaine de 5 à 200 MPa, *Bulletin BNM*, 1982, No. 48, pp. 9-33
9. J.C. Legras, Pressure distortion coefficient of pressure balances, in: *Advances in high pressure science and technology*, *Proc. of the 2nd Intern. Pressure Metrology Workshop & Intern. Conf. on high pressure science and technology*, edited by A.K. Bandyopadhyay et al., NPL New Delhi, India, November 26-30, 2001, pp. 9-14
10. P. Delajoud, The pressure multiplier – a transfer standard in the range 100 to 1000 MPa, *BIPM Monograph 89/1 on High Pressure Metrology Seminar*, 24-25 May 1988, Paris, edited G.F. Molinar, pp. 114-124
11. J. Jäger, W. Sabuga, Establishment of a primary standard for the 1 GPa range of pressure measurement, in: *Advances in high pressure science and technology*, *Proc. of the 2nd Intern. Pressure Metrology Workshop & Intern. Conf. on high pressure science and technology*, edited by A.K. Bandyopadhyay et al., NPL New Delhi, India, November 26-30, 2001, pp. 15-20
12. P. Vergne, New high pressure viscosity measurements on di(2-ethylhexyl) sebacate and comparison with previous data, *High Temperatures – High Pressures*, 1990, vol. 22, pp. 613-621
13. Viscosity and density of over 40 lubricating fluids of known composition at pressures to 150000 psi and temperatures to 425 F, ASME Report, American Society of Mechanical Engineers, New York, NY, USA, 1953